

## Surface magnetic microstructure of melt-spun magnetic ribbons

E. A. Seddon

*Daresbury Laboratory, Daresbury, Warrington WA4 4AD, United Kingdom*

Y. B. Xu and D. Greig

*Department of Physics, The University of Leeds, Leeds LS2 9JT, United Kingdom*

I. R. M. Wardell, D. Rubio-Temprano, and M. Hardiman

*Department of Physics and Astronomy, The University of Sussex, Brighton BN1 9QH, United Kingdom*

Scanning electron microscopy with polarization analysis (SEMPA) and photon-excited spin polarized secondary electron spectroscopy have been used to study respectively the lateral variations and depth profiles of the surface magnetic microstructure of as-cast amorphous melt-spun  $\text{Fe}_{80}\text{B}_{20}$  ribbons. The  $5\ \mu\text{m}$  resolution SEMPA images showed very similar complex domain patterns for both remanent and field-on states, and spot mode hysteresis loops showed significant differences across the sample. These data are consistent with a very wide distribution of strain-induced anisotropy fields. Energy resolved hysteresis loops (ERHL) measured using photoemitted 1 and 20 eV secondary electrons showed clear differences in form, attributable to changes in probing depth. A unidirectional anisotropy found in the 20 eV ERHL is linked tentatively to the inhomogeneities revealed by SEMPA. © 1997 American Institute of Physics.

[S0021-8979(97)35608-4]

Our recently reported spin-resolved photoemission measurements on melt-spun  $\text{Fe}_{80}\text{B}_{20}$ <sup>1</sup> left some unanswered questions relating to the magnetic homogeneity of the sample in the as-cast state and after surface cleaning. Although a number of domain imaging studies has been made in the past on these materials, mostly on field annealed samples,<sup>2</sup> with more recent attention being paid specifically to strain-induced effects,<sup>3</sup> the potential influence of inhomogeneous magnetic microstructure on electron spectroscopy data has yet to be fully appreciated.

We have now investigated the surface magnetism of amorphous melt-spun  $\text{Fe}_{80}\text{B}_{20}$  by measuring the spin polarization of the secondary electron (SE) emission in two complementary experiments that give different degrees of lateral and depth resolution. Scanning electron microscopy with polarization analysis (SEMPA)<sup>4</sup> was used for lateral resolution but since a relatively large spread of SE energies are accepted, the magnetic information is averaged over a range of depths. To obtain a greater degree of depth resolution, we used photon-excited spin polarized secondary electron spectroscopy (SPSES) in which the spin analysis is made on SEs with well-defined kinetic energies.

There is still considerable uncertainty about the effective probing depth of low-energy ( $E_k < 5$  eV) SEs. From the ‘‘universal curve’’ predictions of Seah and Dench,<sup>5</sup> it is expected that 1 eV electrons have much higher values of the inelastic mean free path  $\lambda_i$  ( $> 50\ \text{\AA}$ ) than 20 eV electrons, for which  $\lambda_i \sim 4\text{--}5\ \text{\AA}$ . However, a number of overlayer experiments monitoring the attenuation of spin polarized SEs has concluded that while the probing depth in the 20–50 eV range has the Seah and Dench value, the large increase at low  $E_k$  is not observed. A compilation by Siegmann<sup>6</sup> of all the available data from such experiments indicated that in Fe

the relevant depth is only 5–6  $\text{\AA}$  for  $E_k \leq 5$  eV. In contrast, the most recent work of Furukawa and Koike<sup>7</sup> deduces  $\lambda_m \sim 26\ \text{\AA}$  for  $E_k \leq 4$  eV. Nevertheless, despite these uncertainties in the numerical values, raw SPSES data at 1 and 50 eV (Ref. 8) do show marked differences that can only result from significantly different ( $\geq 2$ ) information depths.

All the data were obtained on two samples taken from the same batch of  $\text{Fe}_{80}\text{B}_{20}$  melt-spun ribbon. Since the details of the various experimental arrangements have been given elsewhere,<sup>1,9</sup> only specific operating parameters are given here. In each experiment, the 2.5-mm-wide as-cast ribbons were arranged as closed loops with the ends clamped together (air side out) and these could be magnetized along the longitudinal (roll) axis using coils wound around the ribbon. The SPSES sample was annealed only by the UHV bakeout ( $\sim 160\ ^\circ\text{C}$  for 24 h) whereas the SEMPA sample always remained at room temperature. Subsequent x-ray analysis of the SPSES sample showed it to have retained its amorphous character. Surface cleaning by Ar ion bombardment was carried out prior to each experiment. SEMPA data obtained before and after a supplementary test cleaning cycle showed no significant changes.

A 5 keV electron gun was used to provide a 1 nA primary beam into a  $5\ \mu\text{m}$  spot in the SEMPA rig. The resulting secondary electron emission at energies up to  $\sim 60$  eV was analyzed using a 20 keV retarding field Mott detector (RFMD) to give the longitudinal polarization component  $P_{\text{Long}}$ , which is to a first approximation proportional to the corresponding magnetization component  $M_{\text{Long}}$ .<sup>10</sup> The asymmetry  $A$ , the directly measured parameter in a spin polarimeter, is related to the polarization  $P$  by  $A = PS_{\text{eff}}$  and the SEMPA detector was operated with an effective Sherman function,  $S_{\text{eff}} = 0.14$ . Data were collected as  $128 \times 128$  pixel

$A_{\text{Long}}(x,y)$  images, obtained at a dwell time of 150 ms per pixel, as linescans  $A_{\text{Long}}(x)$  and as fixed position (spot-mode)  $A_{\text{Long}}(I)$  hysteresis loops.

For the SPSES measurements, photons of 110 eV from Station 6.1 on the Daresbury Synchrotron Radiation Source were used to excite the SEs which were energy resolved with a small hemispherical analyzer. The two mutually perpendicular in-plane asymmetry components  $A_{\text{Long}}$  and  $A_{\text{Trans}}$  were measured simultaneously, again using a 20 keV RFMD with  $S_{\text{eff}}=0.12$ . The SPSES data were recorded as energy resolved (asymmetry) hysteresis loops (ERHL),  $A_{\text{Long}}(I)$  and  $A_{\text{Trans}}(I)$ . Due to the extent of the photon beam, these measurements were spatial averages over a  $\sim 1 \times 0.5 \text{ mm}^2$  area in the middle of the ribbon. Supplementary magneto-optical Kerr effect (MOKE) data were taken on the SPES sample. In terms of depth resolution, the 20 eV SPSES data are highly surface sensitive, the 1 eV SE and the SEMPA probe sub-surface magnetism more strongly, and MOKE is essentially a bulk technique.

Figure 1 shows two SEMPA images, from the same area, of the two remanent states of the ribbon, after magnetization parallel (+) and antiparallel (-) to the longitudinal axis. These have been processed such that the white-to-black contrast corresponds to a measured asymmetry change (about a common mean) of  $\Delta A_{\text{Long}} = \pm 3.6\%$ , or of  $\Delta P_{\text{Long}} = \pm 26\%$ . This latter value is close to the maximum polarization expected for this material over the SE distribution collected; hence, the brightness level reflects directly the magnitude of  $M_{\text{Long}}$ , with white and black corresponding to  $\pm M_{\text{sat}}$ . All the structure in these images is due to polarization changes, with no discernible topographic contrast.

Clearly, over a substantial proportion of this imaged area, mainly in the middle of the ribbon, the local  $M_{\text{Long}}$  is fully saturated and exhibits hysteresis loops consistent with domain wall movement (e.g., loop 1.3 mm of Fig. 2). However, it is important to note that the SEMPA images from the corresponding field-on states are almost indistinguishable from the remanent state images. In particular, the extent of the “reverse saturated” regions (those black in the upper panel and white in the lower panel of Fig. 1) remains unchanged, even at magnetizing fields  $> \times 20$  higher than the coercive field of loop 1.3 mm. (This is more easily seen near 0.4 mm in the linescans of Fig. 1.) These relatively large hard regions, of up to  $\sim 200 \mu\text{m}$  in extent, thus indicate strong local anisotropy fields parallel to the long axis which are almost certainly due to residual stresses produced during fabrication.<sup>2</sup> Lower-magnification SEMPA images show a high concentration of such hard regions along the edges of the ribbon, possibly due to transverse compressive residual stress. The spot mode loops of Fig. 2 sample  $\sim 5 \mu\text{m}$  regions and show a variety of forms, some indicating domain rotation, but the coercive fields of any central hysteretic region are always very similar (e.g., loop 1.56 mm).

The unchanging midgrey areas in the images are probably due either to regions with large transverse in-plane local anisotropy fields or to the submicron scale (and therefore below our resolution limit) maze patterns associated with underlying perpendicular anisotropy in the bulk.<sup>11</sup>

The ERHLs for  $\text{Fe}_{80}\text{B}_{20}$  recorded at secondary energies

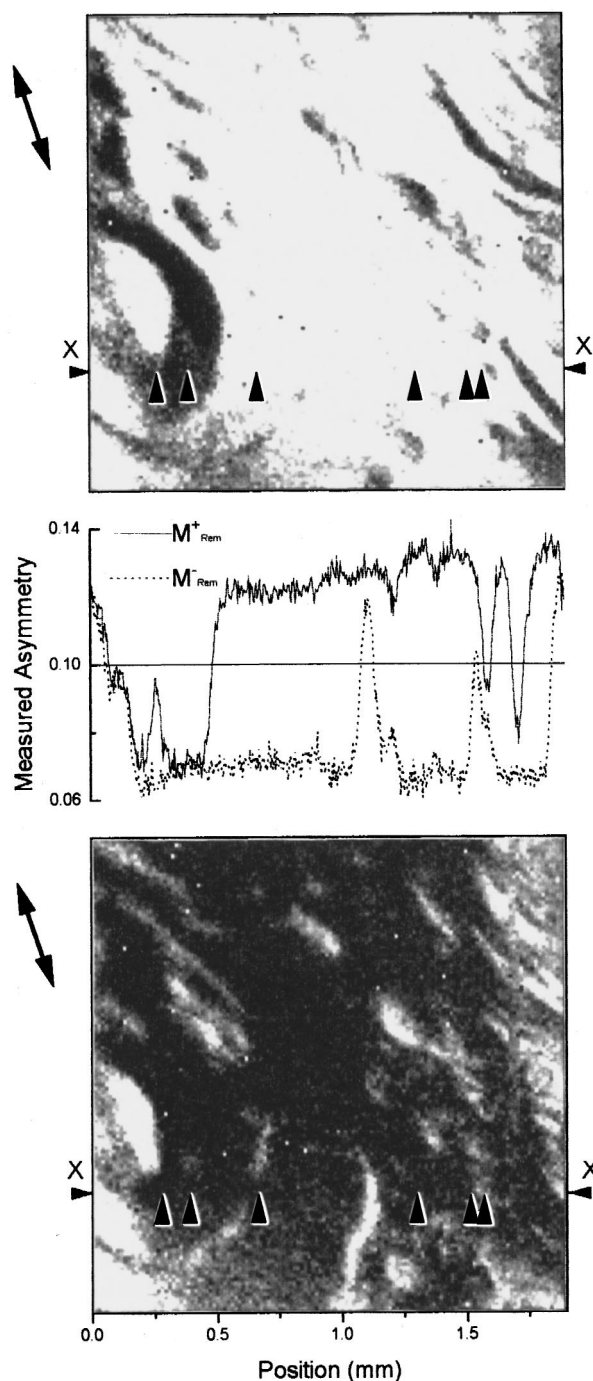


FIG. 1. Upper and lower panels: Remanent state  $A_{\text{Long}}(x,y)$  SEMPA images from an  $\text{Fe}_{80}\text{B}_{20}$  loop after magnetization in the positive and negative longitudinal directions, respectively. Middle panel: Asymmetry line scans  $A_{\text{Long}}(x)$  along line XX for the two states. The longitudinal axis is indicated by the double-headed arrow.

of 1 and 20 eV are presented in Fig. 3. These were both taken from the same area and display variations only in the longitudinal component. The different amplitudes of the ERHLs at 1 eV ( $\Delta P = \pm 17\%$ ) and 20 eV ( $\Delta P = \pm 11\%$ ) are expected from the well-known enhancement of SE polarization at low  $E_k$ , but both are significantly smaller than the largest loops ( $\Delta P = \pm 28\%$ ) seen in the SEMPA data. However, such a reduction is reasonable given the spatial variations in  $M_{\text{Long}}$  revealed by SEMPA and the  $\sim 1 \times 0.5 \text{ mm}^2$  photon beam.

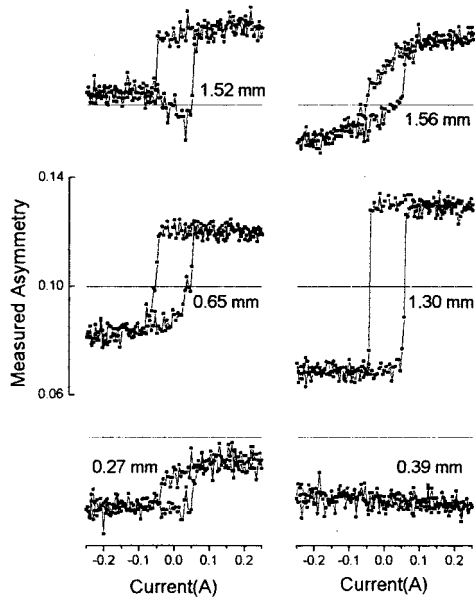


FIG. 2. Spot-mode hysteresis loops  $A_{Long}(I)$  at various points along line XX in Fig. 1 (see arrowheads). The vertical scale is common to all loops and the horizontal lines correspond to  $A=0.1$ .

Generally, the 1 eV ERHL and MOKE loops resemble the square SEMPA ones from homogenous regions of the sample and again this is consistent with the spatial averaging which occurs under photon excitation. The significant rounding of the highly surface sensitive 20 eV loop is similar to that observed by Allenspach *et al.*<sup>8</sup> on an Fe(100) bulk termination.

The values of the mean coercive field  $H_c = (H_c^+ + H_c^-)/2$ , are very similar for both ERHL loops and for those measured in the SEMPA spot mode, but are 20% lower than found using MOKE. This latter finding contrasts with Allenspach *et al.*'s single-crystal data<sup>8</sup> in which  $H_c$  from MOKE had the same value as in both ERHL experiments.

Perhaps the most striking aspect of our ERHL data in Fig. 2 is that the 20 eV loop is shifted along the current (field) axis by about  $0.13H_c$ , indicating unambiguously a mean effective unidirectional anisotropy in the surface layer, at least over the averaged area. Although the spot mode SEMPA loops show a wide variety of shapes, some of which are asymmetric, none exhibit the unidirectional anisotropy of the 20 eV ERHL. We tentatively ascribe this uniaxial anisotropy to an exchange coupling between (i) that part of the longitudinal magnetization that is being reversed by the applied fields used, and (ii) those regions that do not respond (the "reverse saturated" regions of the SEMPA images). This is similar to the well-known exchange anisotropy,<sup>12</sup> but here requires different areas of positively and negatively magnetized hard regions over the total area being sampled. As the probing depth increases, any such difference is expected to average to zero and with it the unidirectional anisotropy.

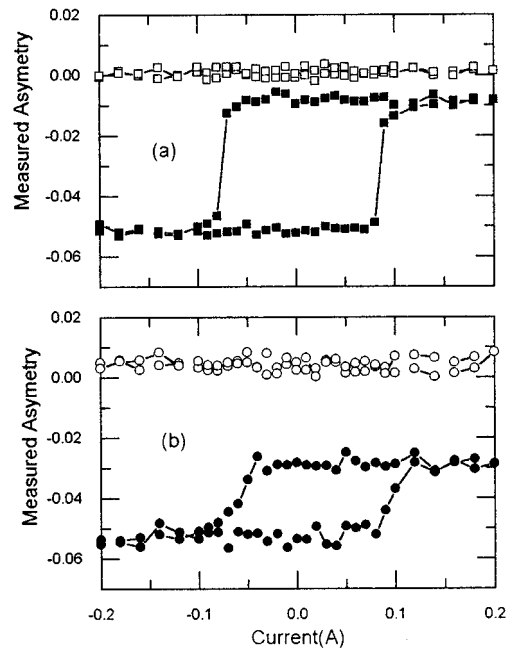


FIG. 3. ERHLs from an  $Fe_{80}B_{20}$  loop recorded at secondary energies of: (a) 1 eV and (b) 20 eV. Solid symbols: longitudinal component; open symbols: transverse component. (The vertical offsets between the data from the two components are instrumental effects.)

The near-surface magnetic structure of amorphous  $Fe_{80}B_{20}$  melt-spun ribbon in the as-cast state is shown to be complex, even in the apparently "saturated" magnetic state (as measured by broad beam techniques). Large scale lateral inhomogeneities and a qualitatively different surface region are found. We have also seen very similar behavior in a variety of Fe and Co based amorphous ribbons and suggest, therefore, that particular care must be exercised in the quantitative interpretation of spin-resolved electron emission data on such samples.

*Acknowledgments:* The authors gratefully acknowledge financial assistance provided by the EPSRC, the ORS, and The University of Leeds. We should like to thank Professor J. A. D. Matthew and Dr. M. R. J. Gibbs for many useful communications and our special thanks go to J. Turton for his skilled technical help.

- <sup>1</sup>Y. B. Xu, C. G. H. Walker, D. Greig, E. A. Seddon, I. W. Kirkman, F. M. Quinn, and J. A. D. Matthew, *J. Phys., Condens. Matter* **8**, 1567 (1996).
- <sup>2</sup>J. D. Livingston and W. G. Morris, *J. Appl. Phys.* **57**, 3555 (1985).
- <sup>3</sup>W. J. Tseng, K. Koike, and J. C. M. Li, *J. Mater. Res.* **8**, 775 (1993).
- <sup>4</sup>M. R. Scheinfein, J. Unguris, M. H. Kelley, D. T. Pierce, and R. J. Celotta, *Rev. Sci. Instrum.* **61**, 2501 (1990).
- <sup>5</sup>M. P. Seah and W. A. Dench, *Surf. Interface Anal.* **1**, 2 (1979).
- <sup>6</sup>H. C. Siegmann, *J. Electron Spectrosc. Relat. Phenom.* **68**, 505 (1994).
- <sup>7</sup>T. Furukawa and K. Koike, *Surf. Sci.* **347**, 193 (1996).
- <sup>8</sup>R. Allenspach, M. Taborelli, M. Landolt, and H. C. Siegmann, *Phys. Rev. Lett.* **56**, 953 (1986).
- <sup>9</sup>M. Hardiman *et al.*, in *Polarized Electron and Polarized Photon Physics*, edited by H. Kleinpoppen and W. R. Newell (Plenum, New York, 1995), p. 147.
- <sup>10</sup>H. C. Siegmann, *J. Phys., Condens. Matter* **4**, 8395 (1992).
- <sup>11</sup>K. Koike, H. Matsuyama, W. J. Tseng, and J. C. M. Li, *Appl. Phys. Lett.* **62**, 2581 (1993).
- <sup>12</sup>I. S. Jacobs and C. P. Bean, in *Magnetism*, edited by G. T. Rado and H. Suhl (Academic, New York, 1963), Vol. 3, p. 323.